

Fine structure of the exciton band and anisotropic optical constants in scheelite PbWO_4 crystals

Masami Fujita

Japan Coast Guard Academy, Wakaba, Kure 737-8512, Japan

Minoru Itoh, Michihiro Horimoto, and Hiroshi Yokota

Department of Electrical and Electronic Engineering, Faculty of Engineering, Shinshu University, Nagano 380-8553, Japan

(Received 9 January 2002; published 19 April 2002)

Polarized reflectivity spectra of PbWO_4 crystals with scheelite structure have been measured using synchrotron radiation in the energy range up to 30 eV. The measurements are undertaken on (011) cleaved surfaces for the polarizations parallel and perpendicular to the crystal a axis. The spectra exhibit remarkable dichroism in the fundamental absorption region. The dielectric constants for the principal crystal a and c axes are derived from the reflectivity spectra with the application of a Kramers-Kronig relation and an equation of dielectric ellipsoid for uniaxial crystals. Polarization dependence of the reflectivity spectra is investigated in detail in the exciton-band region. It is confirmed that the exciton band peaking at 4.25 eV consists of two components with separation of about 0.1 eV for both polarizations $\mathbf{E}\parallel\mathbf{a}$ and $\mathbf{E}\parallel\mathbf{c}$. The intensity of this doublet structure is stronger for $\mathbf{E}\parallel\mathbf{a}$ than for $\mathbf{E}\parallel\mathbf{c}$. Another band appears at around 5.3 eV for $\mathbf{E}\parallel\mathbf{c}$. Origin of these fine structures in the exciton-band region is discussed on the basis of the recent electronic band calculations of PbWO_4 . For the polarization $\mathbf{E}\perp\mathbf{a}$, an additional structure is observed on the high-energy side of the exciton band, which is attributed to the longitudinal exciton-polariton mode.

DOI: 10.1103/PhysRevB.65.195105

PACS number(s): 71.35.Cc, 78.20.-e, 78.20.Ci

I. INTRODUCTION

Nowadays, lead tungstate (PbWO_4) receives intense attention as a promising candidate for scintillating substance,¹ laser host material,² and oxide ion conductor.³ Especially, its luminescence properties have been investigated extensively after the selection as a scintillator in detectors at the Large Hadron Collider in CERN.⁴ Impurity-doping effects and crystal growth techniques have been studied by many workers to improve scintillating characteristics, such as luminescence efficiency, lifetime, and radiation hardness.^{1,4}

From a scientific aspect, the lead tungstate is also an interesting material because it has two stable crystal structures, tetragonal scheelite type and monoclinic raspate type, under normal conditions. Single crystals of PbWO_4 prepared synthetically crystallize in the scheelite structure. The raspate PbWO_4 is obtained as a natural crystal for the present. The present authors have measured reflectivity and luminescence spectra of both phases.^{5,6} This is the only study on the optical properties of raspate PbWO_4 . In recent years, the energy-band structures of several tungstate and molybdate crystals having the scheelite or wolframite (raspite) structure have been calculated by the linearized augmented-plane-wave (APW) method⁷⁻⁹ and the discrete variational $X\alpha$ (DV- $X\alpha$) method.^{10,11}

In spite of a large number of investigations on the luminescence characteristics of scheelite PbWO_4 , the basic optical properties of this material, such as reflectivity spectra or dielectric constants, have not been established experimentally until now. For instance, spectral features of the reflectivity spectra reported by several groups^{5,6,12-14} are not mutually consistent. A main reason for this discrepancy is supposed to be due to the difference in polarization of light with respect to the crystal orientation in each measurement, because the scheelite PbWO_4 crystal has a tetragonal struc-

ture belonging to the space group $I4_1/a$ or C_{4h}^6 . Figure 1 depicts the propagation of the light incident normally on a surface of a uniaxial crystal such as scheelite PbWO_4 , where the optical axis (c axis) makes an angle θ with the normal to the crystal surface. In the crystal, an extraordinary ray with the electric vector parallel to the plane which contains the wave vector \mathbf{k} and the c axis propagates with different velocity from that of an ordinary ray whose electric vector is normal to this plane. In fact, birefringence was observed in the visible region for scheelite PbWO_4 .¹⁵ Very recently, remarkable dichroism in the reflectivity spectra has been observed by us,¹⁶ Kamenskikh *et al.*,¹⁷ and Kirm *et al.*¹⁸ However, there are some serious discrepancies among the results by the different groups.

In this study, polarized reflectivity spectra of scheelite PbWO_4 single crystals have been measured in the energy range from 3 to 30 eV. The polarization dependence in the exciton-band region has been studied in detail. The present

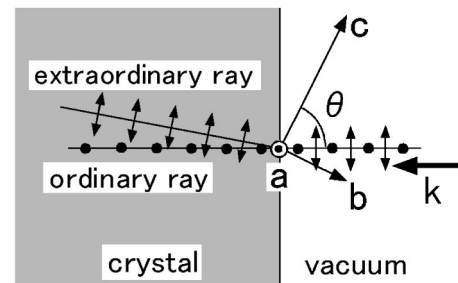


FIG. 1. Propagation of the ordinary ray and the extraordinary ray in scheelite PbWO_4 crystal after the light is incident on the crystal surface under normal configuration. The angle between the optical axis (c axis) and the normal to the surface is represented by θ . The b and c axes and the wave vector \mathbf{k} is in the same plane, while the a -axis is perpendicular to this plane. The electric vector of the extraordinary ray is in the bc plane, while that of the ordinary ray is perpendicular to this plane.

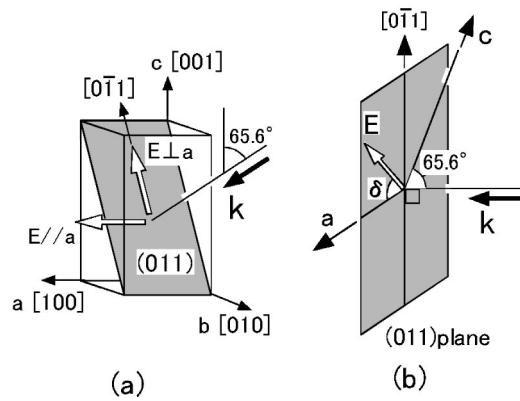


FIG. 2. (a) Experimental arrangement for reflection measurements. Rectangular frame represents the Bravais lattice of scheelite PbWO_4 . Reflection surface of the (011) plane is indicated by the gray plane. Open arrows indicate the polarization directions of the electric vectors of the incident light parallel ($\mathbf{E}\parallel\mathbf{a}$) and perpendicular ($\mathbf{E}\perp\mathbf{a}$) to the a axis. The angle between the c axis and the normal to the (011) plane is 65.6° . (b) Relationship between the polarization of incident light and the crystal axis for the measurement of polarization dependence on the (011) plane. The angle between the polarization direction and the a axis is represented by δ .

experiment provides definitive results on the anisotropic properties of scheelite PbWO_4 . The dielectric constants for the principal crystal axes are calculated using a Kramers-Kronig transformation and an equation of dielectric ellipsoid. It is confirmed that the exciton band peaking at 4.25 eV consists of two components for both polarizations $\mathbf{E}\parallel\mathbf{a}$ and $\mathbf{E}\parallel\mathbf{c}$. An additional structure ascribable to the longitudinal exciton-polariton mode is observed for the polarization $\mathbf{E}\perp\mathbf{a}$. The intensity of the exciton doublet structure for $\mathbf{E}\parallel\mathbf{a}$ is stronger than that for $\mathbf{E}\parallel\mathbf{c}$. Another band appears at around 5.3 eV for $\mathbf{E}\parallel\mathbf{c}$. Origin of these fine structures in the exciton-band region is discussed on the basis of the recent electronic band calculations of PbWO_4 .

II. EXPERIMENT

Single crystals of scheelite PbWO_4 were obtained from the Institute of Solid State Physics of Russian Academy of Sciences and the Materials Research Laboratory of Furukawa Company. They were grown by the Czochralski technique. The cleaved surfaces with typical size of $5 \times 5 \text{ mm}^2$ were used for the reflection measurement. The crystal orientation was confirmed by the x-ray analysis, and checked by means of a pair of crossed polarizers. Polarized reflectivity spectra were measured for more than ten samples. The arrangement for reflection measurements is shown in Fig. 2(a). The rectangular frame represents the Bravais lattice of scheelite PbWO_4 . The crystals are cleaved along the $\{101\}$ plane.¹⁹ As indicated by a gray plane in Fig. 2(a), we took the cleaved surface as the (011) plane, which is one of the equivalent $\{101\}$ planes. The angle between the c axis and the normal of the (011) plane is $\theta = 65.6^\circ$.

The experiments in a wide spectral range up to 30 eV were carried out by using synchrotron radiation of UVSOR facility at the Institute for Molecular Science, Okazaki. The

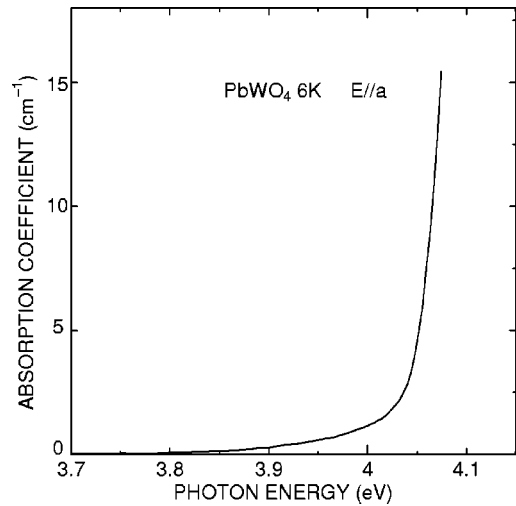


FIG. 3. Absorption spectrum of a cleaved crystal of scheelite PbWO_4 at 6 K for $\mathbf{E}\parallel\mathbf{a}$.

light beam was monochromatized through a 1-m Seya-Namioka monochromator at beam line 1B. The oriented crystals were mounted on the sample holder in a variable-temperature cryostat of He-flow type. The electric vector of the incident light was parallel to the $[100]$ direction ($\mathbf{E}\parallel\mathbf{a}$) or parallel to the $[0\bar{1}1]$ direction which is perpendicular to the a axis ($\mathbf{E}\perp\mathbf{a}$) as shown in Fig. 2(a).²⁰ The incident light with the former polarization propagates as an ordinary ray in the crystal, while that with the latter polarization propagates as an extraordinary ray. Reflectivity spectra were measured under the configuration of near-normal incidence. Polarization dependence of the reflectivity spectra was examined in detail at Shinshu University, in which the light beam from a 150-W D_2 lamp was dispersed with a Jobin-Yvon HR320 monochromator. In this case, the reflectivity spectra up to 5.7 eV were measured for various directions of the polarization by rotating a polarizer installed between the monochromator and the sample.

III. RESULTS

A. Reflectivity spectra

Before presenting the reflectivity spectra, we show the absorption spectrum of a PbWO_4 crystal in Fig. 3. The spectrum was measured at 6 K for the polarization $\mathbf{E}\parallel\mathbf{a}$. A steep absorption starts at 4.05 eV. The energy band calculation in Ref. 7 indicates that the scheelite PbWO_4 crystal has an indirect band gap, which is approximately 0.1 eV smaller than the direct gap. No appreciable steplike phonon structure characteristic of the indirect transition is seen. Therefore, the band gap of PbWO_4 is considered to be of direct type. However, if the indirect gap is very close to the direct gap as predicted in Ref. 7, it is hard to conclude whether the smallest band gap is direct or indirect from Fig. 3. Recently, we investigated the temperature dependence of the fundamental absorption tail of PbWO_4 , and found that the Urbach rule holds for this material.²¹

Figure 4 shows typical reflectivity spectra of PbWO_4 at 8 K up to 30 eV for $\mathbf{E}\parallel\mathbf{a}$ and $\mathbf{E}\perp\mathbf{a}$. The reflectivity in the

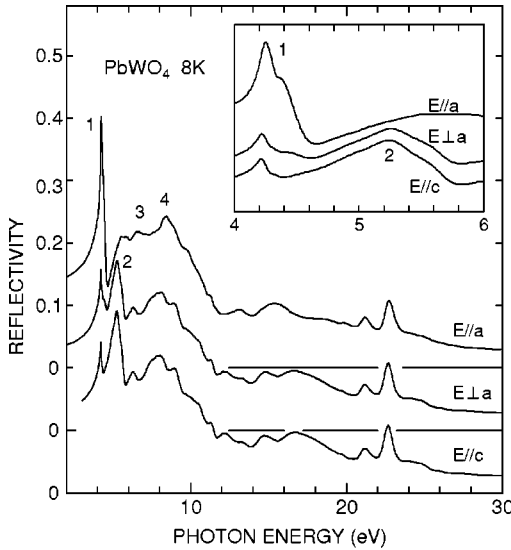


FIG. 4. Reflectivity spectra of scheelite PbWO_4 observed at 8 K for $\mathbf{E}\parallel\mathbf{a}$ and $\mathbf{E}\perp\mathbf{a}$, along with the spectrum derived for $\mathbf{E}\parallel\mathbf{c}$. The spectra in the low-energy region are shown in the inset on an expanded scale.

low-energy region was supplemented by the value calculated from the refractive indices.¹⁵ The reflectivity spectrum for $\mathbf{E}\parallel\mathbf{c}$ will be explained later.

In Fig. 4, a sharp exciton band 1 is observed at 4.25 eV for $\mathbf{E}\perp\mathbf{a}$. The intensity of the band 1 for $\mathbf{E}\perp\mathbf{a}$ is very small. Very recently, two other groups have measured the polarization dependence of the reflectivity spectra of PbWO_4 using oriented samples. The result of Ref. 18 agrees qualitatively with ours, that is, the exciton band 1 is stronger for $\mathbf{E}\parallel\mathbf{a}$ than for $\mathbf{E}\perp\mathbf{a}$.²⁰ In Ref. 17, however, band 1 for $\mathbf{E}\perp\mathbf{a}$ is much stronger than that for $\mathbf{E}\parallel\mathbf{a}$.

The present result is consistent with the birefringence measurement by Baccaro *et al.*¹⁵ They found that the refractive index of the ordinary ray is larger than that of the extraordinary ray, because a strong exciton absorption band makes large dispersion in the visible region.

In order to see the spectral variation between $\mathbf{E}\parallel\mathbf{a}$ and $\mathbf{E}\perp\mathbf{a}$, reflectivity spectra on the (011) face were measured by changing the polarization direction of incident light with respect to the crystal orientation. The angle δ shown in Fig. 2(b) was changed from 0° ($\mathbf{E}\parallel\mathbf{a}$) to 90° ($\mathbf{E}\perp\mathbf{a}$) every 10° . The results are shown in Fig. 5, where δ is indicated on the left side of each spectrum. Since the incident light with the polarization of $0^\circ < \delta < 90^\circ$ propagates separately as an ordinary ray and an extraordinary ray in the crystal, the reflectivity R_δ for angle δ is expressed by a superposition of the reflectivities for the ordinary ray $R_{\mathbf{E}\parallel\mathbf{a}}$ and the extraordinary ray $R_{\mathbf{E}\perp\mathbf{a}}$. In fact, it was confirmed that the reflectivity R_δ in Fig. 5 is described by the simple relation

$$R_\delta = R_{\mathbf{E}\parallel\mathbf{a}} \cos^2 \delta + R_{\mathbf{E}\perp\mathbf{a}} \sin^2 \delta. \quad (3.1)$$

The spectrum of an unoriented sample we reported in Ref. 6 shows mixed character of $\mathbf{E}\parallel\mathbf{a}$ and $\mathbf{E}\perp\mathbf{a}$. The reflectivity

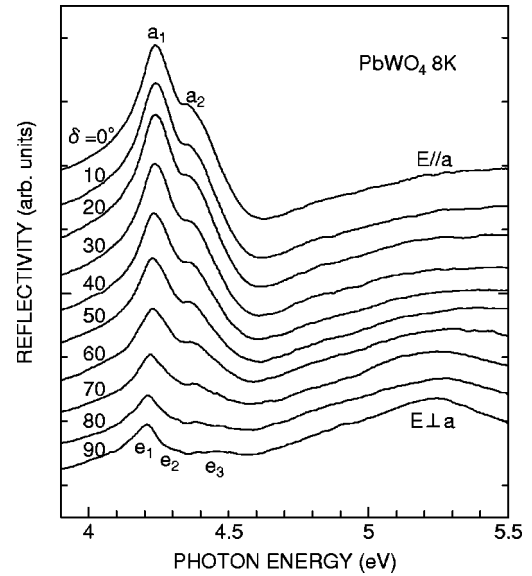


FIG. 5. Polarization dependence of the reflectivity spectra observed in the exciton-band region. The spectra were measured on the (011) cleaved surface. The angle δ (in degrees) between the polarization and the a axis (see Fig. 2(b)) is indicated on the left side of each spectrum.

spectrum reported by Shpinkov *et al.*¹³ resembles the present spectrum for $\mathbf{E}\parallel\mathbf{a}$, although the crystal orientation was not identified.

In Fig. 4, several polarization-dependent structures are also observed in the high-energy region. A strong peak 2 is observed at 5.3 eV for $\mathbf{E}\perp\mathbf{a}$, while such a structure is not observed for $\mathbf{E}\parallel\mathbf{a}$. One may see a shoulderlike structure 3 at 6.5 eV for $\mathbf{E}\parallel\mathbf{a}$ and a weak peak at 6.2 eV for $\mathbf{E}\perp\mathbf{a}$. A broad peak 4 at 8.4 eV ($\mathbf{E}\parallel\mathbf{a}$) and that at 8.0 eV ($\mathbf{E}\perp\mathbf{a}$) probably correspond to the prominent peaks observed in the 8–9 eV region in Refs. 17 and 18. The reflectivity decreases gradually above 9 eV, and shows a minimum at around 12–14 eV. At 11.3 eV is observed a weak peak, which was assigned to the transition from $\text{Pb}^{2+} 6s$ band.⁶ Several sharp peaks originating from the $\text{Pb}^{2+} 5d$ core level are observed in the 19–25 eV region.^{22,23}

We measured polarized reflectivity spectra in the temperature range from 8 to 300 K. The spectral width of the exciton band became broad with increasing temperature. On the other hand, the peak positions of the fine structures in the exciton-band region were found to be almost independent of temperature.

B. Optical constants

Optical properties of PbWO_4 can be described in terms of the complex dielectric constants ϵ^a ($\equiv \epsilon^{xx}$), ϵ^b ($\equiv \epsilon^{yy}$), and ϵ^c ($\equiv \epsilon^{zz}$) with respect to the three principal crystal axes. Here, we use superscripts to express the components of the dielectric tensor, following Ref. 9, and take the a , b , and c axes along the x , y , and z directions, respectively. Note that $\epsilon^a = \epsilon^b$, since the a and b axes are equivalent in scheelite PbWO_4 .

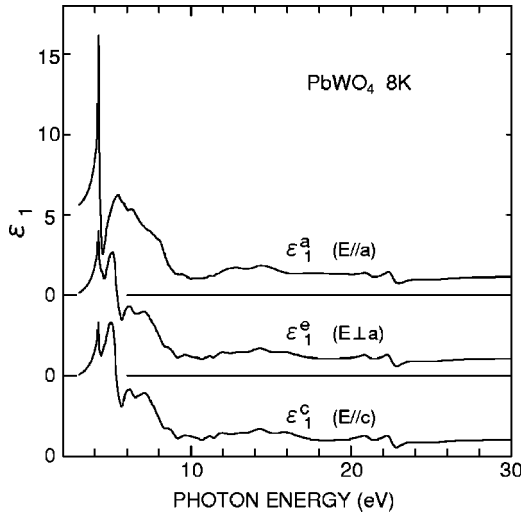


FIG. 6. Real part of the dielectric constant of PbWO₄ for $\mathbf{E}\parallel\mathbf{a}$, $\mathbf{E}\perp\mathbf{a}$, and $\mathbf{E}\parallel\mathbf{c}$ at 8 K.

We take the crystal axes as shown in Fig. 1, that is, the b and c axes and the wave vector \mathbf{k} are in the same plane, while the a axis is perpendicular to this plane. The dielectric constant ε^a is derived through the Kramers-Kronig transformation of the reflectivity spectra for polarization $\mathbf{E}\parallel\mathbf{a}$ in Fig. 4. The real (ε_1^a) and imaginary (ε_2^a) parts of ε^a obtained by this way are shown in Figs. 6 and 7, respectively. As recognized from Fig. 2(a), ε^a represents the dielectric constant for the ordinary ray. On the other hand, the light with $\mathbf{E}\perp\mathbf{a}$ polarization propagates as the extraordinary ray in the crystal. The dielectric constant ε^e for this extraordinary ray is also calculated by the Kramers-Kronig transformation of the reflectivity spectrum for $\mathbf{E}\perp\mathbf{a}$ in Fig. 4. The results of ε_1^e and ε_2^e are depicted in Figs. 6 and 7, respectively.

We further calculated the dielectric constant ε^c as follows. The dielectric constant ε^e for the extraordinary ray shown in Fig. 1 is related to ε^a and ε^c as a function of the angle θ by the equation of dielectric ellipsoid²⁴

$$\frac{1}{\varepsilon^e} = \frac{\cos^2\theta}{\varepsilon^a} + \frac{\sin^2\theta}{\varepsilon^c}. \quad (3.2)$$

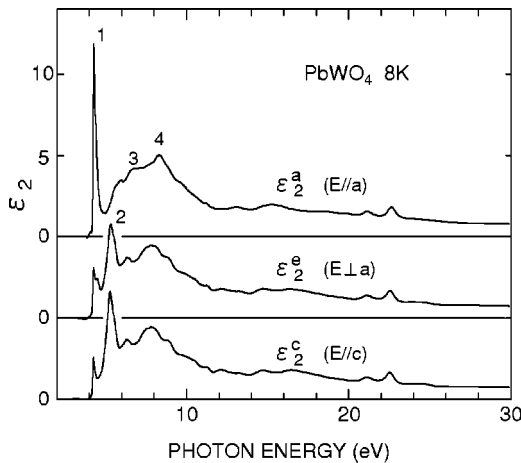


FIG. 7. Imaginary part of the dielectric constant of PbWO₄ for $\mathbf{E}\parallel\mathbf{a}$, $\mathbf{E}\perp\mathbf{a}$, and $\mathbf{E}\parallel\mathbf{c}$ at 8 K.

TABLE I. Energy positions (in eV) of the main structures in the ε_2 spectra of scheelite PbWO₄ at 8 K.

Polarization		$\mathbf{E}\parallel\mathbf{a}$	$\mathbf{E}\perp\mathbf{a}$	$\mathbf{E}\parallel\mathbf{c}$
Structures	1	4.265	4.255	4.250
		4.390	4.340	4.355
	2		4.500	
			5.32	5.28
3	6.62	6.30	6.30	
	4	8.32	7.80	7.82

In the present case, the dielectric constant ε^c is derived with use of this equation, substituting the experimental values into ε^a and ε^e , and taking the angle θ to be 65.6°. The real and imaginary parts of ε^c thus obtained are given in Figs. 6 and 7, respectively. Peak positions of the main structures in the ε_2 spectra are summarized in Table I.

The reflectivity spectrum for $\mathbf{E}\parallel\mathbf{c}$ calculated from ε^c is given in Fig. 4. The absorption coefficients for $\mathbf{E}\parallel\mathbf{a}$ and $\mathbf{E}\parallel\mathbf{c}$ were also calculated from ε^a and ε^c , respectively. The results are shown in Fig. 8. It is worthwhile noting that the $\mathbf{E}\parallel\mathbf{c}$ spectra cannot be observed directly as far as one uses the cleaved surface. They correspond to the spectra which will be obtained by the measurements with the light of normal incidence, if we can prepare good quality surface parallel to the c axis.

The oscillator strength f of an absorption band between the energy E_1 and E_2 per molecule can be calculated by the formula

$$f = \frac{2m}{Ne^2h^2} \int_{E_1}^{E_2} E' \varepsilon_2(E') dE', \quad (3.3)$$

where m is the electron mass, N the number of molecules per unit volume, e the electron charge, h the Planck constant, and

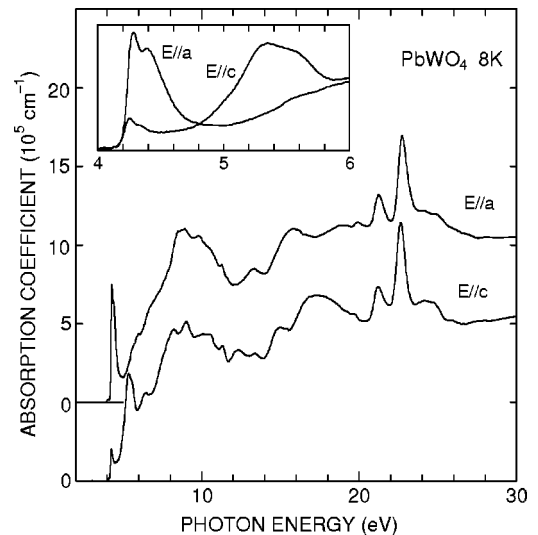


FIG. 8. Absorption coefficient of PbWO₄ at 8 K for $\mathbf{E}\parallel\mathbf{a}$ and $\mathbf{E}\parallel\mathbf{c}$. The spectra in the low-energy region are shown in the inset on an expanded scale.

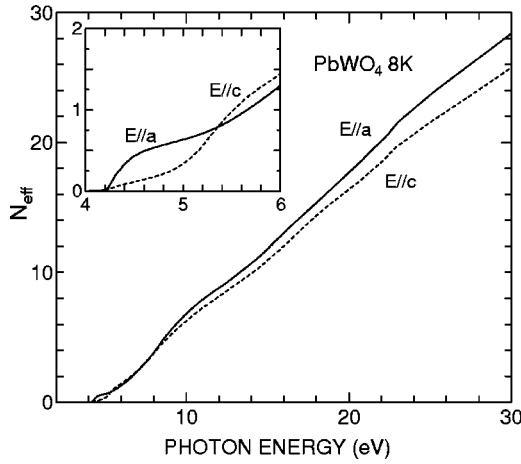


FIG. 9. Effective number N_{eff} of electrons per molecule of PbWO_4 for $\mathbf{E}\parallel\mathbf{a}$ (solid curve) and $\mathbf{E}\parallel\mathbf{c}$ (dotted curve).

E the photon energy. For the exciton band 1 between 4.1 and 4.6 eV, the oscillator strength is estimated to be 0.50 for $\mathbf{E}\parallel\mathbf{a}$, while it is less than 0.10 for $\mathbf{E}\parallel\mathbf{c}$. The magnitude for $\mathbf{E}\parallel\mathbf{a}$ is comparable with that of the exciton band in alkali halides, typical ionic crystals; e.g., the value of f is nearly 0.5 in NaCl and KCl.^{25,26} We get $f \approx 0.55$ for the peak 2 between 4.8 and 5.8 eV for $\mathbf{E}\parallel\mathbf{c}$, subtracting the contribution from the background absorption.

Furthermore, the effective number N_{eff} of electrons per molecule was calculated using the relation

$$N_{\text{eff}}(E) = \frac{2m}{Ne^2\hbar^2} \int_0^E E' \varepsilon_2(E') dE'. \quad (3.4)$$

The result is shown in Fig. 9.

C. Fine structures in the absorption-edge region

As seen from Figs. 4 and 5, the exciton band 1 consists of two or three fine structures. In the upper part of Fig. 10 are shown the ε_2 spectra in the low-energy region on an expanded scale. The exciton band shows doublet structure labeled a_1 and a_2 for ε_2^a and c_1 and c_2 for ε_2^c . We can see a peak e_1 and a hump e_3 for ε_2^a . A weak structure e_2 is also seen in between e_1 and e_3 . The structures e_1 and e_2 are supposed to be the counterparts of c_1 and c_2 , respectively. On the other hand, no structure is found at the position of e_3 in the ε_2^a nor ε_2^c spectra.

It should be noted that the structure e_3 is observed in the spectra of the extraordinary ray which propagates in the off-axis direction in PbWO_4 . In polariton picture, the transverse and longitudinal modes of an exciton-polariton are mixed with each other when its propagation vector does not coincide with any of the principal axes in an anisotropic crystal.²⁷ The lower part of Fig. 10 shows the electron energy-loss functions $-\text{Im}(1/\varepsilon)$ for $\mathbf{E}\parallel\mathbf{a}$ and $\mathbf{E}\parallel\mathbf{c}$, which were calculated from the ε^a and ε^c spectra, respectively. The peaks in the energy-loss spectra correspond to the excitation of longitudinal exciton polaritons. It appears that the energy position of the structure e_3 for ε_2^a is only slightly lower than the peak of

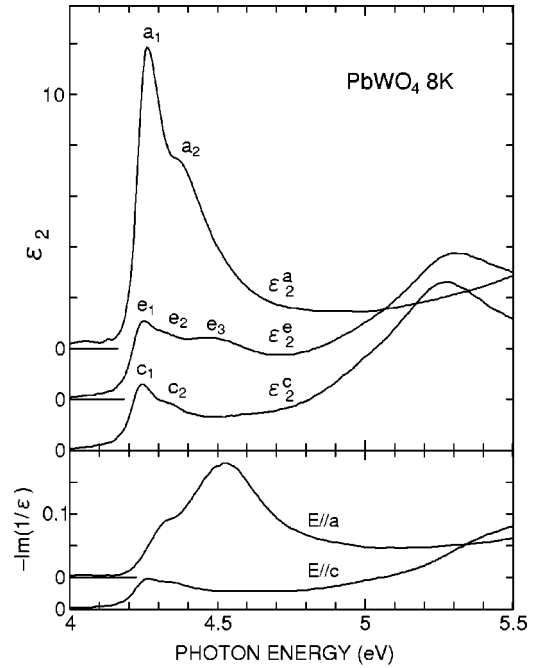


FIG. 10. The ε_2 spectra (upper part) and the electron energy-loss functions $-\text{Im}(1/\varepsilon)$ (lower part) in the exciton-band region.

$-\text{Im}(1/\varepsilon)$ for $\mathbf{E}\parallel\mathbf{a}$. This suggests that the structure e_3 arises from the longitudinal exciton-polariton mode peculiar to anisotropic crystals.

IV. DISCUSSION

A. Overall structure above the band gap

The electronic structure of scheelite PbWO_4 has been calculated using the LAPW method by Zhang *et al.*⁷ The upper part of the valence band consists mainly of the $\text{O}^{2-}2p$ state and the conduction band is dominated by the $\text{W}^{6+}5d$ state. The $\text{Pb}^{2+}6s$ state contributes throughout the valence band. Similar result has been obtained from the DV- $X\alpha$ calculation by Ye *et al.*¹⁰ and by Inabe and Itoh.¹¹ The number of the valence electrons per molecule is 26, which comes from the $6s$ state of one Pb^{2+} ion and the $2p$ state of four O^{2-} ions. In general, the effective number N_{eff} of electrons does not exceed the number of valence electrons below the onset of the transition from an outermost core level, although some exceptions have been known.^{28,29} The present result follows this general case, i.e., $N_{\text{eff}} \approx 16-17$ at 20 eV lower than the $\text{Pb}^{2+}5d$ core level for both polarizations, as shown in Fig. 9.

In order to obtain the optical constants, Zhang *et al.*⁸ have calculated the joint density-of-state (DOS) on the basis of their energy band calculation. From Fig. 2 in Ref. 8, we see that (1) the value of ε_2 just above the band edge is much larger for $\mathbf{E}\parallel\mathbf{a}$ than for $\mathbf{E}\parallel\mathbf{c}$, (2) a distinct peak is observed for $\mathbf{E}\parallel\mathbf{c}$ in the 4–5 eV region, while it is absent for $\mathbf{E}\parallel\mathbf{a}$, and (3) some strong peaks appear at about 7.5 eV for both polarizations. These features reproduce well the overall structure in Fig. 7, if we assume that the calculated band-gap energy is about 1 eV smaller than that of the experimental one.

The present ε_2 spectra show a minimum around 12 eV. We attribute the structures in the 4–10 eV region to the transitions from the valence band to the bottom of the conduction band, because the calculated width of the valence band is about 5.5 eV.⁷ The structures in the 19–25 eV region are apparently due to the transition from Pb^{2+} $5d$ core level. Similar structures have been observed in the optical spectra of lead halides, and explained well on the basis of the cationic $5d \rightarrow 6p$ transition.^{22,23}

B. Exciton structure

The calculation of the joint DOS by Zhang *et al.*⁸ does not include the excitonic effect. Nevertheless, their result of ε_2 shows a sharp singularity of DOS at the band edge. The present experiment reveals that the exciton band of PbWO_4 has a doublet structure for each principal crystal axis. According to their argument, the high-energy structure is assigned to the calculated singularity of DOS, and the low-energy structure to the exciton state associated with this singularity, which means that the exciton binding energy of PbWO_4 is small (~ 0.1 eV).

Although the argument by Zhang *et al.*⁸ is appealing, there are some problems on their calculated result near the band gap. First, no clear symptom of indirect transition is found in Fig. 3, although their calculation indicates indirect band gap.⁷ Some inaccuracy may be included in the calculation of the DOS at the band edge, because the DOS is sensitive to the dispersion of both the valence and conduction bands. Second, the contribution of the Pb^{2+} $6p$ state to the bottom of the conduction band is negligible in their calculation,⁷ from which they pointed out that the Pb^{2+} $6s \rightarrow 6p$ exciton model is not appropriate. However, the DV- $X\alpha$ calculations^{10,11} indicate that the Pb^{2+} $6p$ and W^{6+} $5d$ states have comparable contribution to the bottom of the conduction band. This is consistent with our observation of the Pb^{2+} $5d \rightarrow 6p$ transition at around 23 eV. Therefore, the exciton transition in PbWO_4 would involve the cationic excitation, as well as the charge transfer from oxygen to tungsten.

In a previous paper,¹⁶ we suggested an assignment on the basis of cationic $6s \rightarrow 6p$ excitation picture. A Pb^{2+} ion is in the site of S_4 symmetry. The Pb^{2+} $6p$ level splits into the p_0 ($=p_z$) (Γ_2) level and the $p_{\pm 1}$ ($= (p_x \pm ip_y)/\sqrt{2}$) ($\Gamma_{3,4}$) level due to the crystal field along the c axis. The latter level is further split by the spin-orbit interaction. This situation is similar to the exciton transition in PbI_2 , a typical example of cationic excitation, where the $6p$ level splits due to the crystal field of D_{3d} symmetry and the spin-orbit interaction.³⁰ The analysis on the exciton structure given in Ref. 30 holds formally for the case of PbWO_4 . The Hamiltonian which describes the $6p$ states is given by

$$H = \begin{pmatrix} \zeta/2 & 0 & 0 \\ 0 & -\zeta/2 & \zeta/\sqrt{2} \\ 0 & \zeta/\sqrt{2} & \Delta E_c \end{pmatrix}, \quad (4.1)$$

where ΔE_c and ζ represent the crystal field splitting between Γ_2 and $\Gamma_{3,4}$ and the spin-orbit coupling constant, respec-

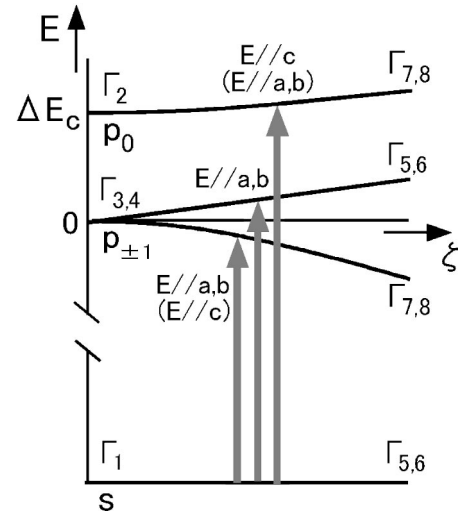


FIG. 11. Schematic energy level diagram of the Pb^{2+} $6s \rightarrow 6p$ transition in the S_4 crystal field. The selection rule is indicated near each solid arrow, while the partially allowed transitions are given in the parentheses.

tively. In Fig. 11 is presented the energy level diagram calculated from Eq. (4.1). The selection rule of the electric-dipole allowed $s \rightarrow p$ transition is given in this figure, where the partially allowed transitions due to weak spin-orbit interaction are given in the parentheses.

According to the abovementioned model, the peaks a_1 and c_1 are assigned to the transition from the ground $\Gamma_{5,6}$ state to the lowest excited $\Gamma_{7,8}$ state, and the peak a_2 is assigned to the transition to the excited $\Gamma_{5,6}$ state. Structure 2, which is strongly observed only for $\mathbf{E} \parallel \mathbf{c}$, is assigned to the transition to the higher excited $\Gamma_{7,8}$ state. Therefore, the model can explain the dichroism of the main structures in the exciton-band region.

The values of ΔE_c and ζ ($=2\lambda$ in Ref. 30) are estimated to be 0.9 and 0.1 eV, respectively, from the energy separation of the fine structures. The corresponding values in PbI_2 have been given as $\Delta E_c = 0.8$ eV and $\zeta = 0.6$ eV.³⁰ Although the crystal structures are different from each other, the larger value of ΔE_c in PbWO_4 seems reasonable, considering that the distance between Pb and the nearest neighbor O in PbWO_4 is 2.58 Å, which is smaller than the Pb-I distance of 3.21 Å in PbI_2 . The value of ζ in our model is small compared to that of PbI_2 . Since there is a considerable hybridization of W^{6+} $5d$ state with the Pb^{2+} $6p$ state in the conduction band in PbWO_4 , the spin-orbit coupling of the $6p$ electron is expected to be reduced. The reason for a small difference in peak positions of a_1 (a_2) and c_1 (c_2) is not clear. There are two possible explanations for this, however. One is ascribed to the anisotropy of the Coulomb and exchange interactions, as proposed for the exciton band of BiI_3 .³¹ The other is due to the Davydov-type splitting, since two molecules are contained in a primitive unit cell of scheelite PbWO_4 .³²

V. SUMMARY

We have measured polarized reflectivity spectra of scheelite PbWO_4 using oriented single crystals. Remarkable

dichroism is found in the optical spectra, especially in the exciton-band region. The optical constants for the principal crystal axes were obtained by using the Kramers-Kronig relation and the equation of the dielectric ellipsoid. The main features observed in the optical spectra were compared with the theoretical energy-band structure. Cationic excitation model in the uniaxial crystal field was applied to explain the main features near the absorption edge.

We would like to notice that special care should be taken when impurity-doping or radiation-damage effects of PbWO_4 crystals are studied experimentally. In these studies, such effects have been discussed by measuring any change in absorption spectrum.⁴ The optical anisotropy would superim-

pose spurious influence on the spectral change due to impurity doping or radiation damage, if the spectra measured with different polarizations are compared with each other.

ACKNOWLEDGMENTS

It is a pleasure to acknowledge the cooperation of Dr. D. L. Alov and Dr. Y. Usuki for supplying the single crystals and Mr. H. Kunisaki and Mr. N. Mozumi for taking the reflectivity data. We would like to express our sincere thanks to Professor M. Kamada and Mr. M. Hasumoto for their help under the Joint Studies Program at UVSOR facility of the Institute for Molecular Science.

- ¹M. Nikl, *Phys. Status Solidi A* **178**, 595 (2000).
- ²W. Chen, Y. Inagawa, T. Omatsu, M. Tateda, N. Takeuchi, and Y. Usuki, *Opt. Commun.* **194**, 401 (2001).
- ³S. Takai, K. Sugiura, and T. Esaka, *Mater. Res. Bull.* **34**, 193 (1999).
- ⁴For recent works, see *Proceedings of the Fifth International Conference on Inorganic Scintillators and Their Applications*, edited by V.V. Mikhailin (M.V. Lomonosov Moscow State University, Moscow, 2000).
- ⁵M. Itoh, D.L. Alov, and M. Fujita, *J. Lumin.* **87-89**, 1243 (2000).
- ⁶M. Itoh and M. Fujita, *Phys. Rev. B* **62**, 12 825 (2000).
- ⁷Y. Zhang, N.A.W. Holzwarth, and R.T. Williams, *Phys. Rev. B* **57**, 12 738 (1998).
- ⁸Y.C. Zhang, N.A.W. Holzwarth, R.T. Williams, and M. Nikl, in *Proceedings of the Third International Conference on Excitonic Processes in Condensed Matter (EXCON'98)*, Boston, 1998, edited by R.T. Williams and W.M. Yen (Electrochemical Society, Pennington, NJ, 1998), p. 420.
- ⁹Y. Abraham, N.A.W. Holzwarth, and R.T. Williams, *Phys. Rev. B* **62**, 1733 (2000).
- ¹⁰X. Ye, C. Shi, C. Guo, X. Yang, and L. Guo, *J. Electron Spectrosc. Relat. Phenom.* **101-103**, 637 (1999).
- ¹¹Y. Inabe and M. Itoh (unpublished).
- ¹²A.N. Belsky, S.M. Klimov, V.V. Mikhailin, A.N. Vasil'ev, E. Auf-fray, P. Lecoq, C. Pedrini, M.V. Korzhik, A.N. Annenkov, P. Chevallier, P. Martin, and J.C. Krupa, *Chem. Phys. Lett.* **277**, 65 (1997).
- ¹³I.N. Shpinkov, I.A. Kamenskikh, M. Kirm, V.N. Kolobanov, V.V. Mikhailin, A.N. Vasilev, and G. Zimmerer, *Phys. Status Solidi A* **170**, 167 (1998).
- ¹⁴I.A. Kamenskikh, M. Kirm, V.N. Kolobanov, V.V. Mikhailin, P.A. Orekhanov, I.N. Shpinkov, A.N. Vasil'ev, and G. Zimmerer, in *Proceedings of the Fifth International Conference on Inorganic Scintillators and Their Applications*, Moscow, 1999, edited by V.V. Mikhailin (M.V. Lomonosov Moscow State University, Moscow, 2000) p. 326.
- ¹⁵S. Baccaro, L.M. Barone, B. Borgia, F. Castelli, F. Cavallari, I. Dafinei, F. de Notaristefani, M. Diemoz, A. Festinesi, E. Leonardi, E. Longo, M. Montecchi, and G. Organtini, *Nucl. Instrum. Methods Phys. Res. A* **385**, 209 (1997).
- ¹⁶M. Fujita, M. Itoh, M. Horimoto, Y. Usuki, M. Kobayashi, and M. Nikl, *J. Phys. Soc. Jpn.* **70**, 1439 (2001).
- ¹⁷I.A. Kamenskikh, V.N. Kolobanov, V.V. Mikhailin, I.N. Shpinkov, D.A. Spassky, and G. Zimmerer, *Nucl. Instrum. Methods Phys. Res. A* **467-468**, 1423 (2001).
- ¹⁸M. Kirm, L. Jönsson, A. Kotlov, V. Nagirnyi, G. Svensson, M. Åsberg-Dahlborg, and G. Zimmerer, in *Proceedings of the Ninth International Symposium on the Physics and Chemistry of Luminescent Materials, Phoenix, Arizona, 2000* (unpublished).
- ¹⁹M. Ishii, K. Harada, M. Kobayashi, Y. Usuki, and T. Yazawa, *Nucl. Instrum. Methods Phys. Res. A* **376**, 203 (1996).
- ²⁰In Refs. 17 and 18, the terms “ $\mathbf{E}\parallel\mathbf{c}$ ” and “ $\mathbf{E}\perp\mathbf{c}$ ” have been used. They correspond to “ $\mathbf{E}\perp\mathbf{a}$ ” and “ $\mathbf{E}\parallel\mathbf{a}$ ” in the present paper, respectively. However, the term “ $\mathbf{E}\parallel\mathbf{c}$ ” is inadequate to represent the polarization direction of the measured spectra, since the c axis is not parallel to the cleaved surface of the $\{101\}$ plane, as shown in Fig. 2(a).
- ²¹M. Itoh, H. Yokota, M. Horimoto, M. Fujita, and Y. Usuki, *Phys. Status Solidi B* (to be published).
- ²²M. Fujita, H. Nakagawa, K. Fukui, H. Matsumoto, T. Miyanaga, and M. Watanabe, *J. Phys. Soc. Jpn.* **60**, 4393 (1991).
- ²³M. Fujita, M. Itoh, Y. Bokumoto, H. Nakagawa, D. L. Alov, and M. Kitaura, *Phys. Rev. B* **61**, 15 731 (2000).
- ²⁴M. Born and E. Wolf, *Principles of Optics* (Pergamon, Oxford, 1975).
- ²⁵T. Tomiki, *J. Phys. Soc. Jpn.* **26**, 738 (1969).
- ²⁶T. Miyata, *J. Phys. Soc. Jpn.* **31**, 529 (1971).
- ²⁷J.J. Hopfield and D.G. Thomas, *J. Phys. Chem. Solids* **12**, 276 (1960).
- ²⁸H.R. Philipp and H. Ehrenreich, *Phys. Rev.* **129**, 1550 (1963).
- ²⁹F. Wooten, *Optical Properties of Solids* (Academic Press, New York, 1972) p. 76.
- ³⁰I.Ch. Schlüter and M. Schlüter, *Phys. Rev. B* **9**, 1652 (1974).
- ³¹Y. Kaifu, *J. Lumin.* **42**, 61 (1988).
- ³²The Bravais lattice of scheelite PbWO_4 shown in Fig. 2(a) contains four molecules, but the primitive cell contains two molecules.